Control Design Methodologies for Vibration Mitigation on Wind Turbine Systems

Ragnar Eide and Hamid Reza Karimi

Department of Engineering, Faculty of Engineering and Science University of Agder
Postboks Grimstad
Norway

1. Introduction

The world's energy consumption from the beginning of the industrial revolution in the 18 th. century and until today has increased at a tremendous degree. Since a large part of the energy has come from sources like oil and coal have the negative impacts on the environment increased proportionally. Therefore, more sustainable and climate friendly energy production methods are emphasized among researchers and environmentalists throughout the world. This is the reason why renewable energies, and wind power particularly, have now become an essential part of the energy programs for most of governments all over the world. One example is seen by the outcome of the European Conference for Renewable Energy in Berlin in 2007 where EU countries defined ambitious goals when it comes to the increase in use of renewable energy resources. One of the goals was that by 2020, the EU would seek to get 20% of energy consumption from renewable energies.

Wind power, in conjunction with other renewable power production methods, has been suggested to play a more and more important role in the future power supply (Waltz, 2008) and (Lee & Kim, 2010). One of the reasons for these expectations is the enormous available potential when it comes to wind resources. One of the most comprehensive study on this topic (Archer & Jacobson, 2005) found the potential of wind power on land and near-shore to be 72TW, which alone could have provided over five times the world's current energy use in all forms averaged over a year.

The World Wind Energy Association (WWEA) estimates the wind power investment worldwide to expand from approximately 160 GW installed capacity at the end of 2010 to 1900 GW installed capacity by 2020. One example is from the USA, where the current contribution of electricity from wind power is merely 1,8% in (2009). However, the U.S Department of Energy is now laying a framework to get as much as 20% contribution by the year 2030.

Due to the economical advantages of installing larger wind turbines (WTs), the typical size of utility-scale turbines has grown dramatically over the last three decades. In addition to the increasing turbine-sizes, cost reduction demands imply use of lighter and hence more flexible structures. If the energy-price from WTs in the coming years are to be competitive with other power production methods, an optimal balance must be made between maximum power capture on one side, and load-reduction capability on the other side. To be able to obtain this is a well defined control-design needed to improve energy capture and reduce

dynamic loads. This combined with the fact that maintenance and constant supervision of WTs at offshore locations is expensive and very difficult, which has further increased the need of a reliable control system for fatigue and load reduction. New advanced control approaches must be designed such as to achieve to the 20- to 25-year operational life required by todayŠs machines (Wright, 2004).

In this paper an above rated wind speed (Region III) regulation of a Horizontal Axis Wind Turbine (HAWT) is presented. The first method is Disturbance Accommodating Control (DAC) which is compared to the LQG controller. The main focus in this work is to use these control techniques to reduce the torque variations by using speed control with collective blade pitch adjustments. Simulation results show effects of the control methodologies for vibration mitigation on wind turbine systems.

The paper is organized as follows. Section 2 will be devoted to the modeling phase. The aim is to come up with a simplified state space model of the WT appropriate to be used in the control design in the subsequent sections. The control system design is covered in Section 3. After a historical overview and a state-of-the-art presentation of WT control are the elements involved in the practical control designed merged with a theoretical description of each topic. The model will then be implemented into a simulation model in the in the MATLAB/Simulink environment in Section 4. Finally, the conclusions and further improvement suggestions are drawn in Section 5.

2. Modeling of the wind turbine

2.1 Introduction

There are different methods available for modeling purposes. Large multi-body dynamics codes, as reported in (Elliot & Wright, 2004), divide the structure into numerous rigid body masses and connect these parts with springs and dampers. This approach leads to dynamic models with hundreds or thousands of DOFs. Hence, the order of these models must be greatly reduced to make them practical for control design (Wright & Fingersh, 2008). Another approach is an assumed modes method. This method discretize the WT structure such that the most important turbine dynamics can be modeled with just a few degrees of freedom. Designing controllers based on these models is much simpler, and captures the most important turbine dynamics, leading to a stable closed-loop system (Wright & Fingersh, 2008). The method is for instance used in FAST, a popular simulation program for design and simulation of control system (Jonkman & Buhl, 2005).

This section presents a simplified control-oriented model. In this approach, a state space representation of the dynamic system is derived from of a quite simple mechanical description of the WT. This state space model is totally non-linear due to the aerodynamics involved, and will thus be linearized around a specific operation point. As reported in (Wright & Fingersh, 2008) with corresponding references, good results are obtained by using linearized time invariant models for the control design.

When modeling a WT one may need to combine different models, each representing interacting subsystems, as Figure 1 below depicts. Here we can see how the WT is simplified to consist of the aerodynamic-, mechanical- (drive train), and electric subsystem, and that the blade pitch angle reference and the power reference in this case are controllable inputs.

The WT is a complicated mechanical system with many interconnecting DOF. However, some of the couplings are rather weak and can be neglected (Ekelund, 1997). For instance, the
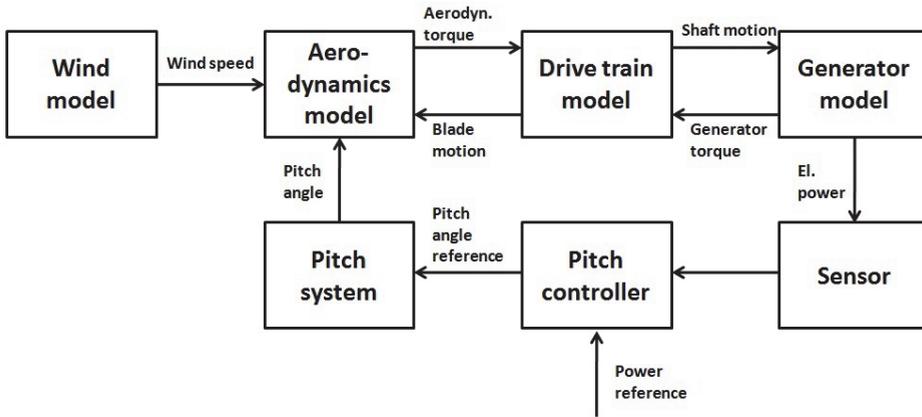
Fig. 1. WT subsystems with corresponding models

connection between the dynamics of the transmission and the tower is neglected in modeling of the mechanical system. The dynamics of the generator and the electrical system are also neglected by regarding the reaction torque from the generator as a fixed value. Also when considering the wind, the approach is to model the wind as simply a scalar input affecting the rotor state.

2.2 State space representation

The nonlinearities of a WT system, for instance due to the aerodynamics, may bring along challenges when it comes to the control design. Since the control input gains of a pitch control usually is the partial derivative of the rotor aerodynamic torque with respect to blade pitch angle variations, these input gains will depend on the operating condition, described by a specific wind and rotor speed. A controller designed for a turbine at one operating point may give poor results at other operating conditions. In fact, a controller which has shown to stabilize the plant for a limited range of operation points, may cause unstable closed-loop behavior in other conditions.

A method which bypasses the challenges of directly involving the nonlinear equations is by using a linear time invariant system (LTI) on state space form. Such a system relates the control input vector u and output of the plant y using first-order vector ordinary differential equation on the form

$$\dot{x} = Ax + Bu + \Gamma u_D$$
$$y = Cx + Du$$
(1)

where x is the system states and matrices A, B, Γ, C and D are the state-, input-, disturbance-, output- and feedthrough- matrix, respectively, and u_D is the disturbance input vector.

The representation of the system as given in Eqns. (1) has many advantages. Firstly, it allows the control designer to study more general models (i.e., not just linear or stationary ODEs). Having the ODEs in state variable form gives a compact, standard form for the control design. State space systems also contain a description of the internal states of the system along with the input-output relationship. This helps the control designer to keep track of all the modes

(which is important to do since a system can be internally unstable, although it is input-output stable). As shall be shown in the following is a description of the dynamics on state-space a good starting point for the further controller and observer designs.

The WT drive-train modeled with its high and low speed shaft separated by a gearbox is shown in Figure 2. As it's seen, the drive train is modeled as a simple spring-damper configuration with the constants K_r and C_r denoting the spring stiffness and damping in the rotor shaft, and similarly; K_g and C_g as representing the spring stiffness and damping in the generator shaft. Figure 2 also shows the inertia, torque, rot. speed and displacement of the rotor and generator shafts. The parameters named as T1, ω_1, q1, N1,I1 are the torque, speed, displacement, number of teeth, and inertia of gear 1, and similarly for gear 2.
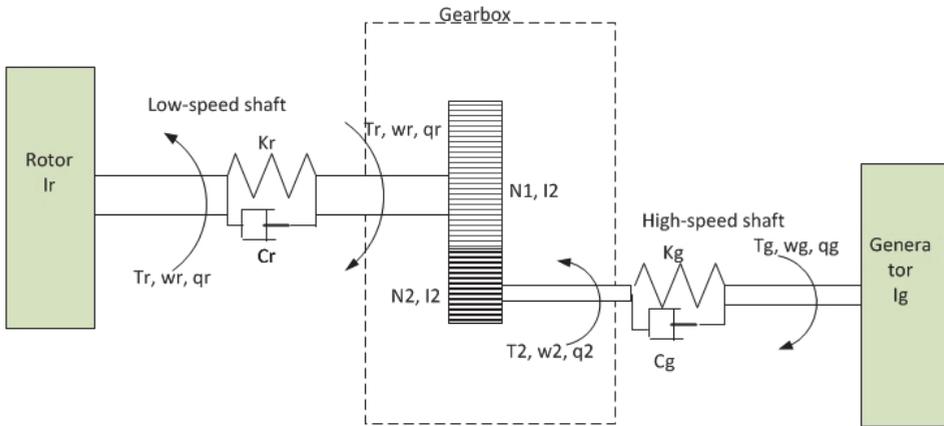

Fig. 2. Model of the drive train with the high and low speed shafts. (For definition of the parameters, see text)

The model in Figure 2 results in the following equation of motion for the rotor torque

$$T_r = I_r \ddot{q}_r + K_r(q_r - q_1) + C_r(\dot{q}_r - \dot{q}_1) + T_1 + I_1 \ddot{q}_1 \tag{2}$$

where the factor $K_r(q_r - q_1) + C_r(\dot{q}_r - \dot{q}_1)$ is the reaction torque in the low speed shaft. Equivalently, the equation for generator motion is as follows

$$T_g = I_g \ddot{q}_g + K_g(q_g - q_2) + C_g(\dot{q}_g - \dot{q}_2) + T_2 + I_2 \ddot{q}_2 \tag{3}$$

where the factor $K_g(q_g - q_2) + C_g(\dot{q}_g - \dot{q}_2)$ is the reaction torque at the high speed shaft. The relationship between T_1 and T_2 is derived based on the equation describing a constrained motion between two gears in the following way

$$\frac{T_2}{T_1} = \frac{\omega_1}{\omega_2} \rightarrow T_1 = \frac{\omega_1}{\omega_2} T_2 \tag{4}$$

From Eqn. (3) we find

$$T_2 = T_g - I_g \ddot{q}_g - K_r(q_g - q_2) - C_r(\dot{q}_g - \dot{q}_2) - I_2 \ddot{q}_2 \tag{5}$$

then, the following equation for the rotor rotation holds

$$T_r = I_r\ddot{q}_r + K_r(q_r - q_1) + C_r(\dot{q}_r - \dot{q}_1) + \frac{\omega_1}{\omega_2}(T_g - I_g\ddot{q}_g - K_r(q_g - q_2) - C_r(\dot{q}_g - \dot{q}_2) - I_2\ddot{q}_2) + I_1\ddot{q}_1 \tag{6}$$

Since the goal of the modeling is to use it for control design, this equation will be simplified in the following. First, it can be assumed that the the high speed shaft is stiff. This will imply that $T_g = T_2$, $\omega_g = \omega_2$ and so on. Secondly, the gearbox can be assumed lossless, hence the terms involving I_1 and I_2 can be omitted. This reduces Eqn. 6 to the following equation

$$T_r = I_r\ddot{q}_r + K_r(q_r - q_1) + C_r(\dot{q}_r - \dot{q}_1) + \frac{\omega_1}{\omega_2}(T_g - I_g\ddot{q}_g) \tag{7}$$

The model is now of three degrees of freedom (DOF); rotor speed, generator speed, and a DOF describing the torsional spring stiffness of the drive train. These DOFs correspond with the three states shown in Figure 3
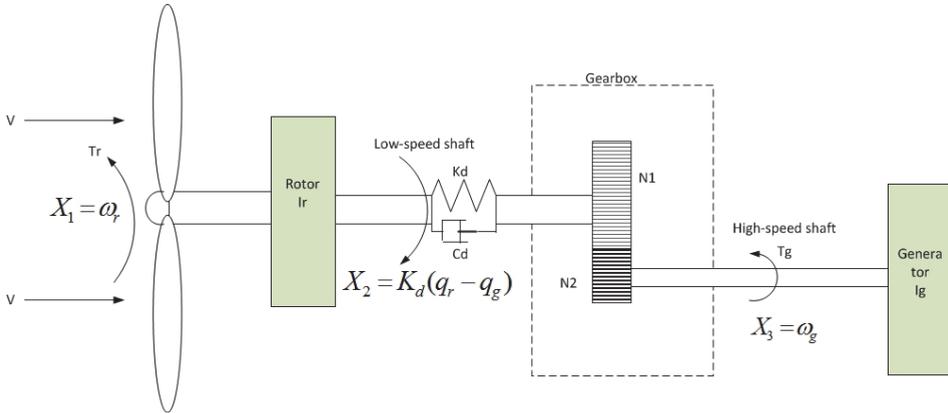

Fig. 3. Illustration of the 3-state model used in the control design having K_d and C_d as drive train torsional stiffness and damping constants, respectively

The states in Figure 3 will in the following be regarded as *perturbations* from an steady-state equilibrium point (operating point), around which the linearization is done. Hence the states are assigned with the δ notation and describes the following DOFs

$X_1 = \delta\omega_r$ is the perturbed rotor speed

$X_2 = K_d(\delta q_r - \delta q_g)$ is the perturbed drive train torsional spring stiffness

$X_3 = \delta\omega_g$ is the perturbed generator speed

where $\delta\dot{q}_r = \delta\omega_r$ and $\delta\dot{q}_g = \delta\omega_g$.
Now, from the Newtons second law, the following relation holds

$$I_r\ddot{q}_r = T_r - T_{sh} \tag{8}$$

where the left hand side expresses the difference between the aerodynamic torque on the rotor caused by the wind force, and the reaction torque in the shaft. This reaction torque can be expressed according to Eqn. (7) as

$$T_{sh} = K_d(q_r - q_g) + C_d(\dot{q}_r - \dot{q}_g) = K_d(q_r - q_g) + C_d(X_1 - X_3) + \frac{\omega_1}{\omega_2}(T_g - I_g\ddot{q}_g) \qquad (9)$$

This equation can, when expressed in terms of deviations from the steady state operation point, be written as:

$$\delta T_{sh} = K_d(\delta q_r - \delta q_g) + C_d(\delta \dot{q}_r - \delta \dot{q}_g) + \frac{\omega_1}{\omega_2}(T_g - I_g\delta\ddot{q}_g) \qquad (10)$$

Hence the BEM theory provides a way to calculate the power coefficient C_P based on the combination of a momentum balance and a empirical study of how the lift and drag coefficients depend on the the collective pitch angle, β, and tip speed ratio, λ . In this way an expression of the aerodynamic torque can be found to be

$$T_r(V, \omega_r, \beta) = \frac{1}{2}\frac{\pi\rho R^2 C_P(\beta, \lambda)}{\lambda}V^2 \qquad (11)$$

where ρ is the air density, R is the rotor radius, and V is the wind speed.
Let us now assume an operating point at $(V_0, \omega_{r,0}, \beta_0)$ such that Eqn. (11) can be written as

$$T_r = T_r(V_0, \omega_{r,0}, \beta_0) + \delta T_r \qquad (12)$$

where δT_r is deviations in the torque from the equilibrium point ($\delta T_r = T_r - T_{r,0}$) and consists of partial derivatives of the torque with respect to the different variables, i.e Taylor series expansion (Henriksen, 2007) and (Wright, 2004), in the following way

$$\delta T_r = \frac{\partial T_r}{\partial V}\delta V + \frac{\partial T_r}{\partial \omega_r}\delta\omega_r + \frac{\partial T_r}{\partial \beta}\delta\beta \qquad (13)$$

where $\delta V = V - V_0$, $\delta\omega = \omega_r - \omega_{r,0}$, and $\delta\beta = \beta - \beta_0$. By assigning α, γ, and ζ to denote the partial derivatives of the torque at the chosen operating point $(V_0, \omega_{rot,0}, \beta_0)$, Eqn. (12) becomes

$$T_r = T_r(V_0, \omega_{r,0}, \beta_0) + \alpha(\delta V) + \gamma(\delta\omega_r) + \zeta(\delta\beta) \qquad (14)$$

If the above expression is put into Eqn.(8), it follows that

$$I_r\ddot{q}_r = T_r(V_0, \omega_{r,0}, \beta_0) + \delta T_r - T_{sh,0} - \delta T_{sh} \qquad (15)$$

At the operation point is $T_r(V_0, \omega_{r,0}, \beta_0) = T_{sh,0}$ since this is a steady state situation. This reduces Eqn. (15) to

$$I_r\ddot{q}_r = \alpha(\delta V) + \gamma(X_1) + \zeta(\delta\beta) - X_2 - C_d(X_1 - X_3) \qquad (16)$$

when substituting with the corresponding state equations. The following expressions for the derivatives of the state variables can now be set up

$$\dot{X}_1 = \frac{(\gamma - C_d)X_1 - X_2 + C_d X_3 + \gamma(\delta\beta) + \alpha(\delta\omega_r)}{I_r} \tag{17}$$

$$\dot{X}_2 = K_d(\delta\dot{q}_r - \delta\dot{q}_g) = K_d X_1 - K_d X_3 \tag{18}$$

$$\dot{X}_3 = \frac{C_d X_1 + X_2 - C_d X_3}{I_g} \tag{19}$$

Note that in the derivative of the generator speed state X_3 is it used that $I_g \ddot{q}_g = I_g X_3 = \delta T_{sh} - \delta T_g = \delta T_{sh}$ when assuming a constant generator torque.

The dynamic system can now be represented in a state space system on the form as described by Eqns (1) yielding

$$\begin{bmatrix} \dot{X}_1 \\ \dot{X}_2 \\ \dot{X}_3 \end{bmatrix} = \begin{bmatrix} \frac{\gamma - C_d}{I_r} & -\frac{1}{I_r} & \frac{C_d}{I_r} \\ K_d & 0 & -K_d \\ \frac{C_d}{I_g} & \frac{1}{I_g} & -\frac{C_d}{I_g} \end{bmatrix} \begin{bmatrix} X_1 \\ X_2 \\ X_3 \end{bmatrix} + \begin{bmatrix} \frac{\zeta}{I_r} \\ 0 \\ 0 \end{bmatrix} \delta\beta + \begin{bmatrix} \frac{\alpha}{I_r} \\ 0 \\ 0 \end{bmatrix} \delta V$$

$$\tag{20}$$

$$y = \begin{bmatrix} 0 & 0 & 1 \end{bmatrix} \begin{bmatrix} X_1 \\ X_2 \\ X_3 \end{bmatrix}$$

where the disturbance input vector u_D from the general form in Eqns. (1) now is given as δV, which is the perturbed wind disturbance (i.e deviations from the operating point, $\delta V = V - V_0$), and the control input vector u from Eqns. (1) now given as $\delta\beta$ (i.e perturbed (collective) pitch angle, $\delta\beta = \beta - \beta_0$).

The parameters will be assigned when coming to Section 4. It is worth no notice that the the measured output signal here is the generator speed. This can be seen from the form of the output vector C. It will be shown later that this will lead to a non-minimum phase plant, i.e a plant with an asymptotically unstable zero in the right complex plane (Lee, 2004). Such plant is in general not suitable for the LTR approach such that a revision of this is required.

3. Wind turbine control

3.1 Introduction
In order to have a power production which ensures that speed, torque and power are within acceptable limits for the different wind speed regions, is it necessary to control the WT. This control system should be complex enough to meet the intended control objectives, but at the same time simple enough to easy interpret the results. A frequently used approach, which will also be applied in this work, is to start with a simple model and a simple controller that can be developed further by adding more degrees of freedom into the model.

Optimally speaking, if the control system shall be able to meet the requirement of reduced energy cost, it must find a good balance between (a) a long working life without failures and (b) an efficient (optimal power output) and stable energy conversion. The first point can be regarded as the main focus in this work. This requirement can be further crystallized to the following properties which the control system should possess

- good closed loop performance in terms of stability, disturbance attenuation, and reference tracking, at an acceptable level of control effort.
- low dynamic order (because of hardware constraints)
- good robustness

To meet the objective of long working life should the control system be designed to be efficiently mitigate loads in order to reduce the fatigue stresses (especially in shaft and blade rotor) due to varying wind disturbances. Before going into the specific control design, an historical overview of WT control with a special view toward the objective of load reduction, will be presented in the following.

3.2 History of WT control

The history of WT control and research within this field have emerged from the simplest form of passive stall control to advanced controllers, like so-called smart rotor control. The latter is well described in for instance (Wilson, Berg, Barone, Berg, Resor & Lobitz, 2009a) and (Lackner & van Kuik, 2010). As these references portrays does this control scheme involve active aerodynamic flow control by implementation of numerous sensors and actuators, bringing along a high level of complexity. Although these advanced control methods have been investigated for ten to fifteen years, most commercial systems are still implemented using multiple single-input-single-output (SISO) loops with classical PID controllers (Bossanyi, 2000). Actually, as reported in (Bossanyi, 2004), PID showed to give competitive results compared to some of the new advanced techniques.

The traditional way of controlling a WT with multiple control objectives, such as speed control for maximum power tracking and load mitigation by pitch control, is to design independent control loops in a way illustrated in Figure 4(a).
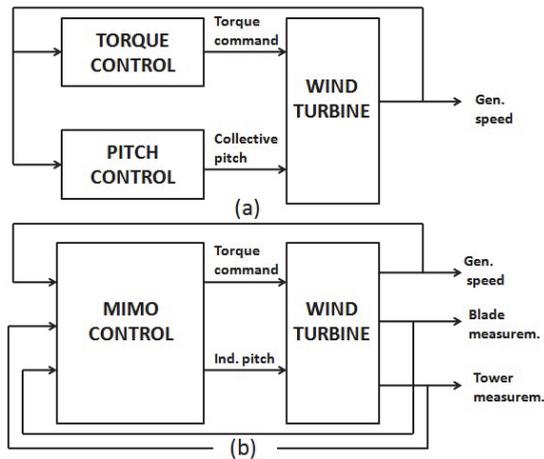

Fig. 4. Illustration of difference between SISO and MIMO controllers

The PID controllers (i.e. the SISO controllers shown in Figure 4 (a)) are traditionally used for the individual torque and pitch control and have shown to have a good effect when carefully tuned and adjusted to its specific application. One disadvantage is, however, that the PID

control loops must be designed not to interfere with each other. If this happen to be the case will the result often be a destabilized turbine. This problem can be solved in an efficient manner within the modern and so-called advanced control techniques (Wright & Fingersh, 2008) using MIMO controllers (cf. Figure 4 (b)). In these more advanced control designs, multiple control objectives is seen to be met with fewer control loops leading to stable closed loop behavior (Wright & Stol, 2008).

With increasing turbine sizes, much research is done to find new and better ways of load control compared to the classical methods (see (Wright & Stol, 2008) and (Bossanyi, 2003) with references). Large turbine sizes will give rise to loads that vary along the blade and change quickly due to wind gusts and other varying wind conditions. Rapidly changing loads can cause fatigue damage and reduce the life of the WT, which in turn may decide the lifetime of the other turbine components. Because of the inertia of the system, as well as the limitations of the actuators, active pitch control alone can only control Şaverageˇ loads on the blade. On the other hand, passive load control strategies cannot respond to local load variations. Active aerodynamic load control (AALC) is therefore suggested to have a good potential as an addition the existing control strategies when it comes to load reduction (Wilson, Berg, Barone, Berg, Resor & Lobitz, 2009b). One approach where AALC has been combined with an individual blade pitch control scheme has shown to reduce the root flap bending moment significantly (Wilson, Berg, Resor, Barone & Berg, 2009).

A well known MIMO controller, the Linear Quadratic Gaussian (LQG) regulator, is suggested in (Selvam, 2007) to be used in load control. This paper presents that this regulation policy can have a good load reduction capability for a large frequency range. Reports as (Bossanyi, 2003) and (Bossanyi, 2004) suggest load mitigation when using individual pitch actuators. A thorough study has been performed by Bossanyi in (Bossanyi, 2003) where the classical PI control is compared with a multi-variable LQG control approach. Although this work has shown to yield good results when applying LQG, the design process is not straightforward and the resulting algorithm is relatively difficult.

One of the disadvantages of LQG design, however, is that it cannot directly take into account robustness margins (like the gain- and the phase margin). Due to this poor robustness properties of LQG control it was been necessary to search after other methods which could handle model uncertainties in a better way. One method which can be traced back to the early 1980s is the H_∞ approach. In this approach does the control designer from the very beginning specify a model of system uncertainties, which can be for instance additive perturbations or output disturbance (D.-W.Gu et al., 2005). Connor, Iyer, Leithead and Grimble were among the first to suggest an application of H_∞ control on a WT model (see Connor et al., 1992). Their main concern in this work were how to reduce the matter of fatigue loading. Although they encountered some overshoot problems did they prove that the method was applicable to a WT control problem. Suggestions of how H_∞ control can be used for load reduction has later been reported in (Bianchi et al., 2004). The method has also been shown to be applicable in advanced power control to enhance a better power capture for a wider range of wind speeds (Liu et al., 2008).

One particular problem the WT control designers must be able to handle is that WT control generally involves a multi-objective optimization problem, each objective having different goals. For instance, the control objective can be alleviate loads due to large scale gusts over the whole disk area, while others can be more slowly varying and low frequency loads over only one blade. To handle this problem does (Bottasso et al., 2010) propose an approach based

on a multi-layer architecture. In this method are three control layers designed, each aiming at a specific control target and cooperates with the other layers to obtain various control goals. In this way, the choice of the controller used on each layer can be optimized and tailored to the specific control goal of that layer, thereby improving performance and simplify tuning (Bottasso et al., 2010).

What the control designer in all of the above mentioned controlling methods are actually trying to do is to compensate for the stochastic fluctuations in the wind. To do this in a perfect way is of course more or less impossible. One method called Disturbance Accommodating Control (DAC) take into account the fluctuations in the wind by an estimation of the disturbance for an assumed above-rated wind speed situation (Balas et al., 1998). DAC has shown to have a good effect on load mitigation and is therefore used to obtain special attention when it comes to fatigue load reduction. The theory was thoroughly compared with PI control by Alan Wright in his PhD thesis from 2004 (Wright, 2004). He concluded in his paper that the analytic results obtained using DAC appeared to be "extremely promising". For instance, it was shown how DAC has much better performance compared to the PI control in reducing drive-train shaft torsional moments and blade root flapwise-bending moments (Wright, 2004). A brief description of the theory behind the DAC will be given shortly, while an implementation and testing of DAC for the WT system will be done in Section 4.

In addition to the above mentioned control schemes are methods as Model Predictive Control (MPC) (Henriksen, 2007), Generalized Predictive Controller (GPC), and Fuzzy Logic Control (Karimi-Davijani et al., 2009) proposed for WT control. A comparison of different control techniques will not be done in this work (please refer to (Bottasso et al., 2007) for more on this).

3.3 The Linear Quadratic Regulator (LQR)

The LQR controller was among the first of the so-called advanced control techniques used in control of wind turbines. Liebst presented in 1985 a pitch control system for the KaMeWa wind turbine using LQR design (Wright, 2004). The objective of this controller was to alleviate blade loads due to wind shear, gravity, and tower deflection using individual blade pitch control. Results of this work included a reduction of blade and tower cyclic responses as well as the reduction of a large 2-per-revolution variation in power (Liebst, 1985).

The practical application of this technique is limited by the challenges of obtaining accurate measurements of the states needed in the controller. One way to solve this is to add extra sensors and measurement arrangements. However, since this extra sensors and measurements will add considerable cost and complexity to a WT, is this most often not regarded as a good solution. In addition, errors in the measurement of these states can result in poor controller behavior (Wright, 2004). To avoid these problems, a state estimator is added in any practical LQR implementation (Laks et al., 2009). This approach was described by Mattson in his Ph.D thesis as early as in 1984, where power-regulation for a fixed-speed WT using blade pitch is presented (Mattson, 1984). The proposed solution to the WT control problem was here based on linear models containing drive-train torsion and tower fore-aft bending DOF. The same report also describes the use of state estimation to estimate wind speed.

The principles of a LQR controller is given in Figure 5. Here the state space system is represented with its matrices A, B, and C, together with the LQR controller (shown with the $-K$).

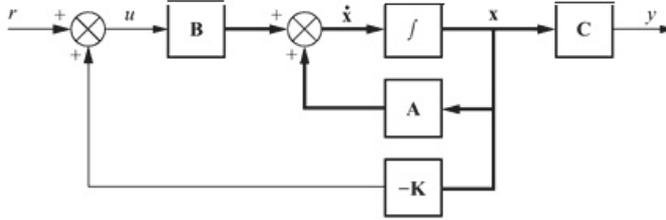The LQR problem rests upon the following three assumptions (Athans, 1981):

Fig. 5. State space control using a LQR controller where K is the LQR gain matrix

1. All the states are available for feedback, i.e it can be measured by sensors etc.

2. The system are *stabilizable* which means that all of its unstable modes are controllable

3. The system are *detectable* having all its unstable modes observable

LQR design is a part of what in the control area is called *optimal control*. This regulator provides an *optimal control law* for a linear system with quadratic performance index yielding a cost function on the form (Burns, 2001)

$$J = \int_0^\infty x^T(t) Q x(t) + u^T(t) R u(t) \, dt \tag{21}$$

where $Q = Q^T$ and $R = R^T$ are weighting parameters that penalize the states and the control effort, respectively. These matrices are therefore controller tuning parameters.

It is crucial that Q must be chosen in accordance to the emphasize we want to give the response of certain states, or in other words; how we will penalize the states. Likewise, the chosen value(s) of R will penalize the control effort u. As an example, if Q is increased while keeping R at the same value, the settling time will be reduced as the states approach zero at a faster rate. This means that more importance is being placed on keeping the states small at the expense of increased control effort. On the other side, if R is very large relative to Q, the control energy is penalized very heavily. Hence, in an optimal control problem the control system seeks to maximize the return from the system with *minimum cost*.

In a LQR design, because of the quadratic performance index of the cost function, the system has a mathematical solution that yields an *optimal control law* given as

$$u(t) = -Kx(t) \tag{22}$$

where u is the control input and K is the state feedback gain matrix given as $K = R^{-1}B^T S$. It can be shown (see (Burns, 2001))that S can be found by solving the following algebraic Riccati Equation (ARE)

$$SA + A^T S + Q - SBR^{-1}B^T S = 0 \tag{23}$$

The process of minimizing the cost function by solving this equation can easily be done using the built-in MATLAB function `lqr`.

As can be seen from the above description does the LQR algorithm take care of the tedious work of optimizing the controller, which for the case of the PID controller can be a time consuming task. However, the control designer still needs to specify the weighting factors

and compare the results with the specified design goals. This means that controller synthesis will often tend to be an iterative process where the designed "optimal" controllers are tested through simulations and will be adjusted according to the specified design goals.

The optimal control solution from the LQR approach yields some impressive properties. Firstly the controller guarantees at least 60° phase margin in each input channel (Saberi et al., 1993), which means that as much as 60° phase changes can be tolerated in each input channel without violating the stability. In addition, the LQR has infinite gain margin which implies that the LQR is still able to guarantee the stability, even though the gain increases indefinitely. Hence, LQR guarantees a very robust controller, capable of handling various kinds of uncertainties in the modeling. However, when an state estimator is implemented with measurement feedback, these properties just described is often lacking. But, as will be shown later; the robustness properties can be recovered!

3.4 State estimation

As mentioned for the case of the LQR controller, all sensors for measuring the different states are in this case assumed to be available. This is not a valid assumption in practice. A void of sensors means that all states (full-order state observers), or some of the states (reduced order observer), are not immediately available for use in the control task. In such cases, a state observer must be implemented to supply accurate estimations of the states at all wind-rotor positions. The observer state equations are given by

$$\dot{\hat{x}} = A\hat{x} + Bu + L(y - C\hat{x}) \tag{24}$$

$$\hat{y} = C\hat{x} \tag{25}$$

where $\hat{x}$ is the estimate of the actual state x. Furthermore, equations (24) and (25) can be re-written to become

$$\dot{\hat{x}} = (A - LC)\hat{x} + Bu + Ly \tag{26}$$

These are the governing equations for a *full order observer*, having two inputs u and y and one output, $\hat{x}$. Since we already know A, B, and u, observers of this kind is simple in design and provides accurate estimation of all the states around the linearized point. The proportional observer gain matrix, L, can be found for instance by pole placement procedure, or as will be shown in the following; by applying the Kalman filter design.

3.5 Kalman estimator

In the previous design of the state observer, the measurements $y = Cx$ were assumed to be noise free. This is not usually the case in practical life. Other unknown inputs yielding the state equations to be on the general stochastic state space form, which is already defined in Eqn. (1) as

$$\dot{x} = Ax + Bu + \Gamma u_D$$

$$y = Cx + Du + n$$

here the D matrix relating the input u to the output y most commonly is set to zero, the disturbance input vector u_D is stationary, zero mean Gaussian white process noise (i.e wind disturbance), and n is zero mean Gaussian white sensor noise.

The Kalman filter can be applied to yield the estimated state vector $\hat{x}$ and output vector $\hat{y}$ (cf. Eqns (24) and (25), by using the known inputs u and the measurements y. The Kalman filter is optimal in the sense that it minimizes the estimated error covariance when some presumed conditions are met (see Bottasso & Croce 2009). The mean-square estimation error is given by

$$J = E[(x(t) - \hat{x}(t))^T (x(t) - \hat{x}(t))] \tag{27}$$

where

$$E[(x(t) - \hat{x}(t))^T y(t)] = 0 \tag{28}$$

The optimal Kalman gain is given by

$$L(t) = S_e(t) C^T R^{-1} \tag{29}$$

where $S_e(t)$ is the same as J given in (3.5). Furthermore, when $t \to \infty$, the algebraic Riccati equation can be written as

$$0 = S_e A^T + A S_e + Q_n - S_e C^T R_n^{-1} C S_e \tag{30}$$

where Q_n and R_n are the process and measurement noise covariances, respectively. Tuning of the Kalman filter are required if these are not known. Finally, the sub-optimal Kalman gain for a steady state Kalman filter can be expressed as $L = S_e C^T R^{-1}$.

3.6 Disturbance accommodating control

This section will explain the principles of DAC and for more details, please refer to e.g. (Johnson, 1976). The DAC method will be utilized together with a LQR regulator and is a straightforward way to model and simulate a system with an assumed-wind disturbance.

Recalling from the state space system described by Eqns. (1), which included the vector Γ. This vector describes the magnitude of the disturbance, while the input signal u_D is the disturbance quantity (which in our case is the wind speed perturbation). The Γ vector will in the DAC procedure be used as a free design parameter.

The basic thought in DAC theory is that disturbances are described by an assumed-waveform model on state space form. Such a wind model can be described according to the following equations (Wright, 2004)

$$\dot{z}_D = F z_D \tag{31}$$
$$u_D = \Theta z_D \tag{32}$$

where z_D denotes the disturbance state, F the state matrix, u_D is disturbance output vector (input to the plant), and Θ relates disturbance model input to disturbance states. Note that it is necessary to know something about the initial condition of the disturbance state, z_D^0, in order to know the amplitude of the disturbance.

Since the state variables x and the disturbance variable z_D cannot be measured directly, observers will be utilized to estimate these. The mathematical description of the observer

will in this case according to Eqns (24) and (25) be given as

$$\dot{x} = A\hat{x} + Bu + \Gamma\hat{u}_D + K_x(y - \hat{y}) \tag{33}$$

$$\hat{y} = C\hat{x} \tag{34}$$

where the estimator gains K_x can be chosen according to for instance the pole placement method using the `place` command in MATLAB.

Furthermore, the disturbance observer is described as

$$\dot{\hat{z}}_D = Fz_D + K_D(y - \hat{y}) \tag{35}$$

$$\hat{u}_D = \Theta\hat{z}_D \tag{36}$$

where the disturbance state estimator gain K_D is a scalar.

The estimated variables can then be fed into the controller to minimize the effect of the disturbances. The result of this is that the state feedback now also include the feedback of disturbance observer yielding a "new" feedback control law on the form

$$u(t) = G\hat{x}(t) + G_D\hat{z}_D(t) \tag{37}$$

where the LQR gain G is computed in MATLAB, and the full state feedback gain (i.e disturbance gain) G_D must be chosen as to minimize the norm $|BG_D + \Gamma\Theta|$. Calculated numerical values will be given in Section 4.

3.7 The LQG controller

Another well-known method of handling noise inputs is the Linear Quadratic Gaussian (LQG) controller. This is simply a combination of a Kalman filter and a LQR controller. The separation principle guarantees that these can be designed and computed independently (Morimoto, 1991). LQG controllers can be used both in linear time-invariant (LTI) systems as well as in linear time-variant systems. The application to linear time-variant systems enables the design of linear feedback controllers for non-linear uncertain systems, which is the case for the WT system.

The schematics of a LQG is in essence similar to that depicted in Figure **??** in Section 3.4, the only difference is that the observer gain matrix L in this figure now can be defined as the Kalman gain K_f. However, we also assume disturbances in form of noise, such that the system with the LQG regulator in compressed form can be described as in Figure 6

4. Control design and simulations

4.1 Introduction

The purpose in this project is to investigate the application of modern control theories, such as the LQR and LQG, on WT systems and how a speed controller can be made with these theories to reduce torque variations due to a wind disturbance. In addition, a further idea is to investigate if a better load reduction can be obtained by using a dynamic compensator from the LTR algorithm, and whether factors as the LTR gain will affect this result.

The simulations are done in the MATLAB Simulink environment, enabling the LTI state space model described in Section 2 to be incorporated together with the different controllers in the convenient block diagram approach available in Simulink.
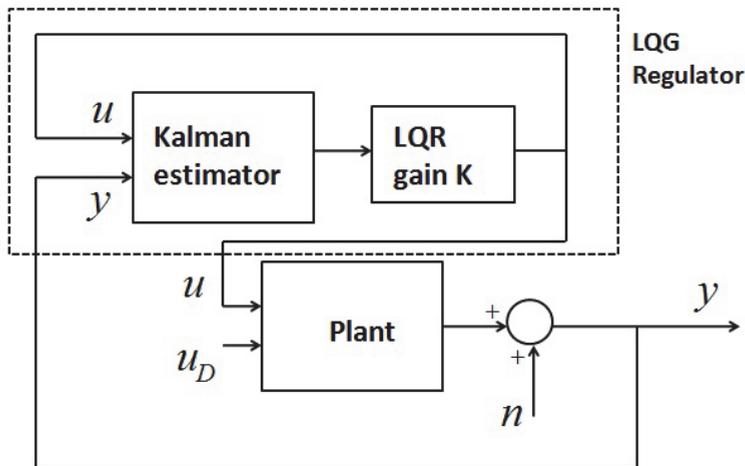
Fig. 6. LQG regulator

This Section presents results from the practical implementation of the WT control design. It is important to note that a test of the controlled system under various operating conditions has not been performed. This is mainly due to the fact that this work is not focused on a real-life application of the controller, but instead on the theoretical aspects of controller design. Also, the linearization of the WT plant at different operation points would have required a computer program, such as FAST[1]. Load mitigation in above rated wind speeds has already been described to be the focus of this work, and the operation point chosen will reflect this goal.

The first control approach that is being tested is the DAC theory, where the wind disturbance modeled in a straightforward way together with the LQR and observer procedures, as described in Section 3. The reason for starting with this method is to investigate if the results are comparable with the results from the LQG method, and if so; what is the difference in the results, and which results can be regarded as the "best" results.

It is important to note that for the simulations in this project are the actuator constraints, such as the dynamics of the pitch-system, not taken into consideration.

4.2 Linearization

As was described in Chaper 2 does the WT compose of a complex non-linear relationship between factors such as the aerodynamic properties of the blades, pitch angle, and wind speeds. The best approach is thus to build the model out from experimental data and a non-linear simulation model of the WT. Although it is possible to build a non-linear WT simulation model also in Simulink and extract linear models by utilizing the built-in `trim` and `linmod` functions, has this not been done in this work. Since the mathematical model presented in this paper is simplified a lot would this approach probably result in a more inaccurate model than with the use of the tailored WT simulation code provided by FAST,

---

[1] A popular aeroelastic design code for horizontal axis wind turbines developed by National Renewable Energy Laboratory, USA (Jonkman & Buhl, 2005)

where many aspects regarding the aerodynamics and structural dynamics are taken into account. The linearized state space model, which will be used in the control design is based on what is presented in (Wright, 2004) and (Balas et al., 1998).

The operation point, around which the linearization is done, is given as (Wright, 2004),

$V_0 = 18m/s$

$\omega_{rot,0} = 42rpm$

$\beta_0 = 12°$

The corresponding FAST linearization with reference to (Wright, 2004) around this point yields the following state space system

$$
\begin{bmatrix} \dot{X}_1 \\ \dot{X}_2 \\ \dot{X}_3 \end{bmatrix} = \begin{bmatrix} -0.145 & -3.108 \cdot 10^{-6} & 0.02445 \\ 2.691 \cdot 10^7 & 0 & -2.691 \cdot 10^7 \\ 0.1229 & 1.56 \cdot 10^{-5} & -0.1229 \end{bmatrix} \begin{bmatrix} X_1 \\ X_2 \\ X_3 \end{bmatrix} + \begin{bmatrix} -3.456 \\ 0 \\ 0 \end{bmatrix} \delta\beta + \begin{bmatrix} 1 \\ 0 \\ 0 \end{bmatrix} (\delta V)
$$

(38)

$$
y = \begin{bmatrix} 0 & 0 & 1 \end{bmatrix} \begin{bmatrix} X_1 \\ X_2 \\ X_3 \end{bmatrix}
$$

where the factors C_d/I_{rot} and C_d/I_{gen} are calculated by using the known relation to the other parameters.

Recalling from Section 2 that Γ vector is given as $\frac{\alpha}{I_r}$, where α is describes the relationship between torque variations and wind variations, $\frac{\partial T_r}{\partial V}$. This means that if Γ is increased, it will follow that the torque is more sensitive to wind variations, which is surely a negative effect when the matter of fatigue is concerned. The torque is given as a non-linear function in Eqn (11), which shows the dependency on the wind speed, rotor speed and blade pitch, and will be fixed at the chosen operating point. However, the Γ vector is initially chosen to $[100]^T$.

The transfer function (TF) of the open loop system formed by the linearized state space system in Eqns. (4.2) is

$$
G(s) = \frac{1.499 \cdot 10^{-14}s^2 - 0.4247s - 1450}{s^3 + 0.374s^2 + 503.3s + 59.44}
$$

(39)

extracted by using the MATLAB function `ss2tf`

One of the zeros of this TF is located at $s = 2.83 \cdot 10^{13}$ leading to a non-minimum phase system. Since the LTR procedure applied as an extension to the LQG later on is not feasible for non-minimum phase systems (Saberi et al., 1993) will this vector be formed as to represent rotor speed measurement instead, which changes the output to

$$
y = \begin{bmatrix} 1 & 0 & 0 \end{bmatrix} \begin{bmatrix} X_1 \\ X_2 \\ X_3 \end{bmatrix}
$$

(40)

4.3 Disturbance accommodating control

The DAC procedure has already been described in Section 3.6. The Simulink block digram shown in Figure 7 was set up according to the governing equations described in this section.
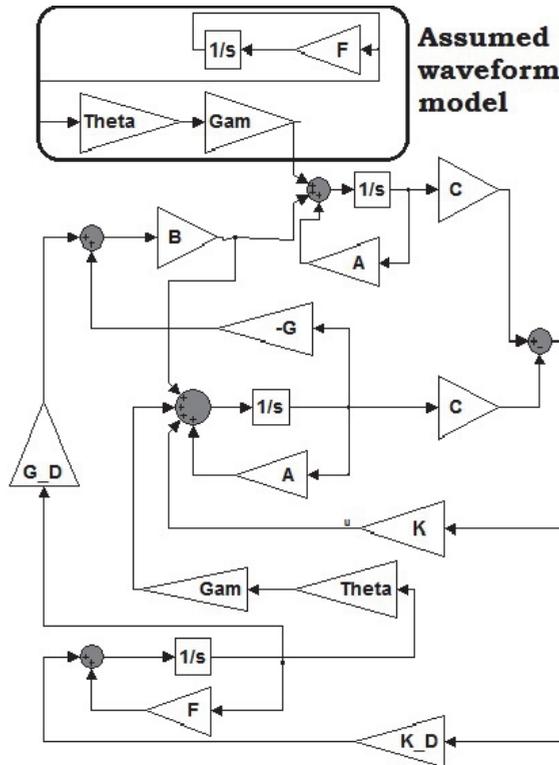
Fig. 7. Simulink block diagram of DAC

The assumed waveform model is shown in Figure 7. It is assumed a step input disturbance from the wind, hence $F = 0$ and $\Theta = 1$ will be chosen to reflect this (Henriksen, 2007). In order to "excite" the controller an initial condition (chosen as 1) were inserted into the integrator of the disturbance model.

4.3.1 Simulation without any control
It is interesting first to have a look at the response without any control at all. Then, after implementing the controller, is it easier to see how good the controller works in the disturbance accommodating task.

Now, by setting both the LQR and the wind disturbance gain equal to zero, perturbations in rotor speed (i.e. deviation from the operation point) shown in Figure 8 when simulating for 50 seconds. According to the simulation result, it is observed that the wind disturbance is not accommodated, and the rotor speed will increase.

4.3.2 Simulation with only wind disturbance gain
The next scenario which is to be simulated is a situation with the LQR control gain set to 0, but with the wind disturbance state gain G_D set to minimize the norm $|BG_D + \Gamma\Theta|$. The response of the rotor speed is shown in Figure 9 below.
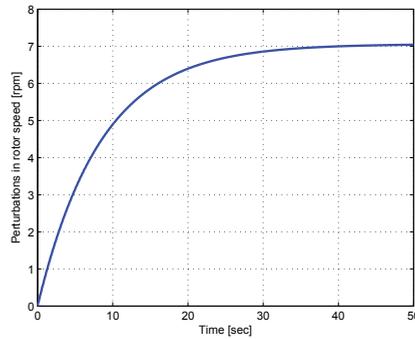
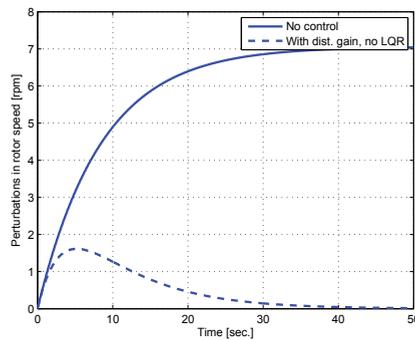Fig. 8. Perturbations in rotor speed with no control

Fig. 9. Perturbations in rotor speed with disturbance gain

As can be seen in this plot does G_D alone manage to regulate the speed, but with a long settling time.

4.3.3 Simulation of DAC with LQR

The final DAC approach will involve a LQR design. Hence, this design will be described in the following, with reference to the theories on LQR presented in Section 3.3. The initial parameters of the wighting functions Q and R are chosen arbitrarily. The next task is then to simulate to check whether the results correspond with the expected performance. After an iterative study while changing Q and R values, the following weighting matrices were chosen:

$$Q = \begin{bmatrix} 100 & 0 & 0 \\ 0 & 0 & 0 \\ 0 & 0 & 100 \end{bmatrix} \tag{41}$$

The control weight of the performance index R was set to 1.

The chosen values in Q will result in a relatively large penalty of the states x_1 and x_3. This means that if x_1 or x_3 is large, the large values in Q will amplify the effect of x_1 and x_3 in the optimization problem. Since the optimization problem are to minimize J, the optimal control u must force the states x_1 and x_3 to be small (which make sense physically since x_1 and x_3

represent the of the perturbations in rotor and generator speed, respectively). On the other hand, the small R relative to the max values in Q involves very low penalty on the control effort u in the minimization of J, and the optimal control u can then be large. For this small R, the gain K can then be large resulting in a faster response.

Since the system has been found to be observable the estimator poles can be arbitrarily placed. Hence, the poles were chosen to be at -10, -30, and -50 yielding the estimator gain matrix

$$K = \begin{bmatrix} 17,235 \\ 1.41 \cdot 10^8 \\ 89.626 \end{bmatrix} \tag{42}$$

The disturbance state estimator gain K_D is a scalar and chosen to 10.

It was found when doing these simulations and checking the results, that an exponential LQR were more appropriate for the current application. The exponential LQR gain were found by applying the code:

```
P=are(A+alpha*eye(3),inv(R)*B*B',Q);
Gdac=inv(R)*B'*P;
```

where alpha is the exponential time-constant chosen to 4. This resulted in the gain matrix:

$$Gdac = \begin{bmatrix} -18.2087 & -1.2265 \cdot 10^{-5} & -0.0425 \end{bmatrix} \tag{42}$$

Simulation of the time response of perturbations in rotor speed for ten seconds is shown in Figure 10.
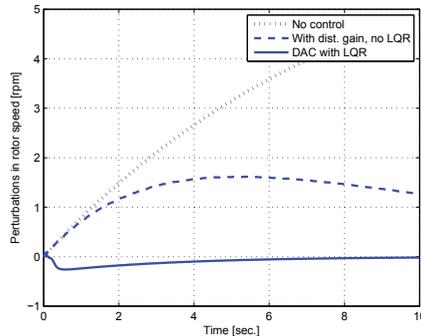

Fig. 10. Comparison of perturbations in rotor speed when applying DAC with LQR

When looking at the plots in Figure 10, it is clear that the disturbance now is much better attenuated while comparing with the first two scenarios. The reason why the speed have this undershoot is due to the right complex plane zeros the LQR controller gives to the closed loop system.

It is also of interest to see how the control signal changes in the three previous situations. This is shown in Figure 11.

As can be seen from Figure 11 does the pitch angle end up having a higher value. This is an expected situation since it is now assumed a constant wind disturbance which must be
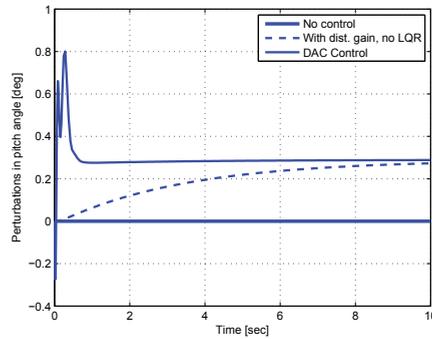
Fig. 11. Comparison of control signal for three previous scenarios

accounted for by an increase in pitch angle. Otherwise, the step in the wind would result in a higher rotor speed, a situation we do not want to occur and the very reason for having a control system in the first place.

Another interesting signal is the error signal, which is the discrepancy between the "measured" output signal y and the estimated signal $\hat{y}$. This is shown in Figure 12 below.
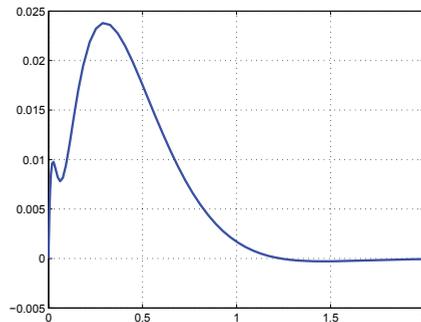

Fig. 12. Error signal for a step input

The DAC simulations in this section have shown that this control method enables to mitigate disturbance due to a wind assigned to affect the rotor state. However, the simulations show that the settling time is relatively long (approximately 10 sec). Whether it is possible to obtained a "better" result using a LQG controller, will be the task in the following section.

The disturbance will now be replaced by two step functions and the disturbance vector Γ in order to make the DAC more comparable with the LQG analysis. This gives the disturbance input signal as shown in Figure 13.

The output response when applying this disturbance model is given in Figure 14

4.4 LQG controller

The control objective is the same as for the DAC; make the perturbations in the rotor speed as small as possible in order to attenuate the wind disturbance. The wind disturbance is made
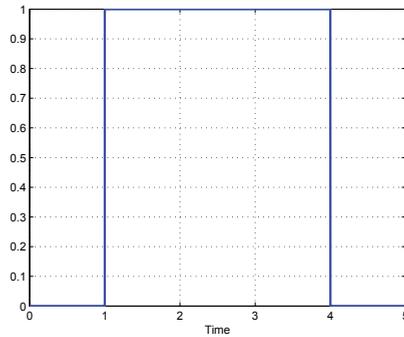
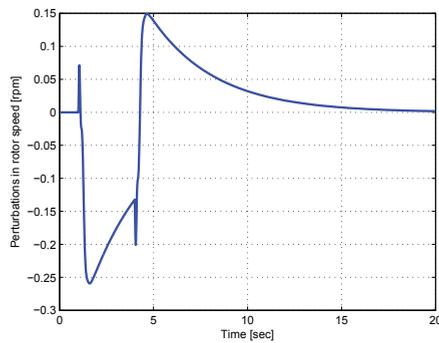Fig. 13. Step signal for disturbance modeling

Fig. 14. Output response when applying step input

by using the combination of two step functions as described earlier. This will give a step input affecting the rotor state. Firstly, a situation without control is showed in Figure 15.
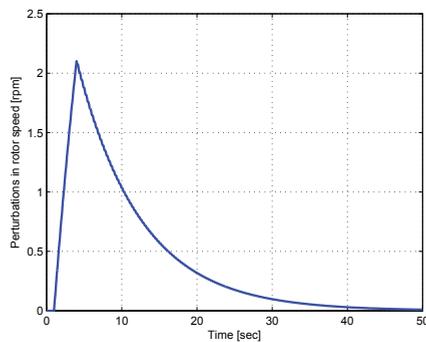

Fig. 15. Response in rotor speed without any control

The sudden change in the rotor speed after one second is due to the step input function. The figure show that without any control will the rotor speed increase to approximately 2 rpm

above the operational speed. After four seconds, when the disturbance is set to zero again, will the speed then decrease and be brought to zero after approximately 50 seconds.

Calculation of the Kalman gain used in the LQG controller is according to the theory discussed in Section 3. There are different methods to do this calculation in MATLAB. One is by applying the `kalman` function, and another is the `lqrc` function. The latter is for instance used in the LTR demo provided with the Robust Control Toolbox in MATLAB. When applying the same weighting as for the LQR in the DAC approach in the `lqrc` function, and the weighting functions

$$Q_n = \begin{bmatrix} 30 & 0 \\ 0 & 30 \end{bmatrix}$$
$$R_n = 1$$

representing the process and measurement noise covariances in the `kalman` function, did the `kalman` function yield much better disturbance attenuation for a given control effort (shown in Figure 16). The corresponding load attenuation for the two cases is shown in Figure 17 below
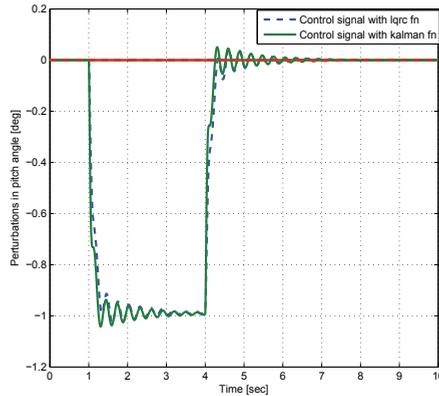

Fig. 16. Comparison of control effort while applying `kalman` and `lqrc` functions in MATLAB

The differences in the output response can be seen through the Kalman gain matrix, which when using the `lqrc` function were calculated to

$$Kf = \begin{bmatrix} 10.38 \\ -1.76 \cdot 10^{-6} \\ -1.65 \end{bmatrix} \tag{40}$$

Similarly, the Kalman gain matrix when using the `kalman` function is

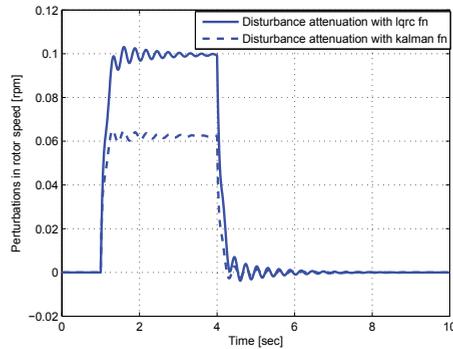$$Kf2 = \begin{bmatrix} 57.60 \\ 3.87 \cdot 10^{-6} \\ 1.07 \end{bmatrix} \tag{40}$$

Fig. 17. Comparison of rotor speed for similar control effort while applying `kalman` and `lqrc` functions in MATLAB

The LQR gains were calculated with an exponential LQR with a time-constant α set to 10, and were given as

$$G = \begin{bmatrix} -25.78 & -2.68 \cdot 10^{-5} & -5.70 \end{bmatrix} \tag{40}$$

The perturbation in rotor speed when comparing the LQG with the DAC response is shown in Figure 18.
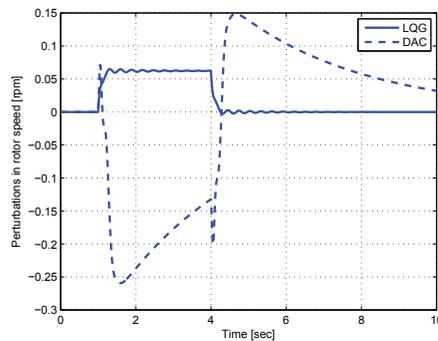

Fig. 18. Comparison of perturbations in rotor speed for LQG and DAC

Figure 18 makes it clear that the effect of the two different control methods is quite different when comparing the two output signals. The LQG controller will not force the disturbance to zero in the same way as the DAC does, which must be regarded as a disadvantage of the LQG. However, the DAC gives a much larger overshoot which is not very positive seen from a controller's perspective.

Similarly, the perturbations in pitch angle for the two methods is shown in Figure 19.

This figure shows that the control effort is much higher for the DAC approach than for LQG. To improve the robustness properties of the LQG will the LTR approach now be introduced as a way to ensure good robustness in spite of uncertainties in the plant model.
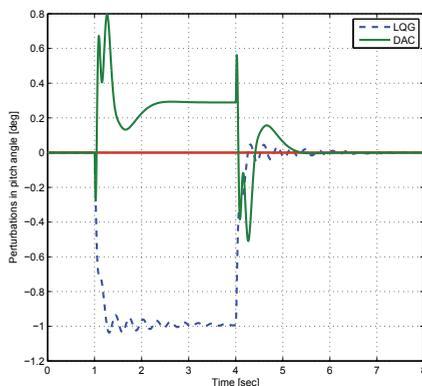
Fig. 19. Comparison of perturbations in pitch angle for the LQG and DAC

5. Conclusions and further works

The purpose of this thesis has been to reduce the loads on a WT for above rated wind speeds (Region III) by speed control when applying different controlling methods. This was first performed by pitch regulation with DAC. This regulation policy showed to have some regulation capacity, but also resulted in some bias in the control signal. It was found when utilizing the DAC controller that although the wind disturbance was well mitigated, the settling time was relatively long(approx. 10 sec). It could have been interesting to extend the work also to include torque regulation in below rated wind speeds. This regulation policy would aim at mitigation of speed and torque variations due to wind disturbances in Region II. The LQG regulator showed to give good speed attenuation, but since DAC and LQG is quite different approaches were a comparison between them not possible. It would have been of major interest to extend the work to also considering pitch actuator constraints to see how this would have affected the results, especially the control input signal.

6. Acknowledgment

7. References

Archer, C. L. & Jacobson, M. Z. (2005). Evaluation of global wind power, *Journal of Geophysical Research* Vol. 110: p. 17.

Athans, M. (1981). The Linear Quadratic LQR problem, *Massachusets Institute of Technology* .

Balas, M., Lee, Y. & Kendall, L. (n.d.). Disturbance tracking control theory with application to horizontal axis wind turbines, *Proceeding of the 1998 ASME Wind Energy Symposium, Reno, Nevada, 12-15 January* pp. 95–99.

Bianchi, F., Mantz, R. & Christiansen, C. (2004). Power regulation in pitch-controlled variable-speed WECS above rated wind speed, *Renewable Energy* Vol. 29(No. 11): pp. 1911–1922.

Bossanyi, E. A. (2000). The design of closed loop controllers for wind turbines, *Wind Energy* Vol.3: pp.149–163.

Bossanyi, E. A. (2003). Individual blade pitch control for load reduction, *Wind Energy* Vol. 6: pp.119–128.

Bossanyi, E. A. (2004). Developments in individual blade pitch control, *EWEA conference-The Science of Making Torque from Wind DUWIND Delft University of Technology April 19-21 2004* .

Bottasso, C. & Croce, A. (2009). Cascading kalman observers of structural flexible and wind states for wind turbine control, *Technical report*, Dipartimento di Ingegneria Aerospaziale, Politecnico di Milano, Milano, Italy.

Bottasso, C., Croce, A., Devecchi, D. & Riboldi, C. (2010). Multi-layer control architecture for the reduction of deterministic and non-deterministic loads on wind turbines.

Bottasso, C., Croce, A. & Savini, B. (2007). Performance comparison of control schemes for variable-speed wind turbines, *Journal of Physics: Conference Series 75, The Science of Making Torque from Wind* .

Burns, R. S. (2001). *Advanced Control Engineering*, Butterworth Heinemann.

Connor, B., Iyer, S., Leithead, W. & Grimble, M. (1992). Control of a horizontal axis wind turbine using H-infinity control, *First IEEE Conference on Control Applications*, pp. 117–122.

Gu D.-W., Petkov P.Hr. & Konstantinov, M. (2005). *Robust Control Design With MATLAB*, Springer.

Ekelund, T. (1997). *Modeling and Linear Quadratic Optimal Control of Wind Turbines*, PhD thesis, Chalmers University of Technology, Gothenburg, Sweden.

Elliot, A. S. & Wright, A. D. (2004). Adams/wt: An industry-specific interactive modeling interface for wind turbine analysis, *Wind Energy* .

Henriksen, L. C. (2007). Model Predictive Control of a Wind Turbine, *Informatics and Mathematical Modelling - Technical University of Denmark* .

Johnson, C. D. (1976). Theory of Disturbance- Accommodating Controllers, *Advances in Control and Dynamic Systems* Vol. 12: pp. 387–489.

Karimi-Davijani, H., Sheikholeslami, A., Livani, H. & Karimi-Davijani, M. (2009). Fuzzy logic control of doubly fed induction generator wind turbine, *World Applied Sciences Journal* Vol. 6 (4): pp. 499–508.

Lackner, M. A. & van Kuik, G. A. M. (2010). The performance of wind turbine smart rotor control approaches during extreme loads, *Journal of Solar Energy Engineering* Vol. 132(No.1).

Laks, J. H., Pao, L. Y. & Wright, A. D. (2009). Control of wind turbines: Past, present, and future, *University of Colorado at Boulder, USA* .

Lee, C.-H. (2004). Stabilization of nonlinear nonminimum phase systems: Adaptive parallel approach using recurrent fuzzy neural network, Vol. 34(No. 2): pp. 1075–1088.

Lee, J. & Kim, S. (2010). Wind power generations impact on peak time demand and on future power mix, *Green Energy and Technology* 3: 108–112.

Liebst, B. (1985). A pitch control system for the KaMeWa Wind Turbine, *Journal of Dynamic Systems and Control* Vol. 107(No.1): pp.46–52.

Liu, J.-H., Xu, D.-P. & Yang, X.-Y. (2008). Multi-objective power control of a variable speed wind turbine based in h infinite theory, *International Conference on Machine Learning and Cybernetics*.

Jonkman & Buhl Jr M.L. (2005). Fast's user guide, *National Renewable Energy Laboratory* .

Morimoto, H. (1991). Adaptive LQG regulator via the Separation Principle, *IEEE Transactions on Automatic Control* VOL. 35(No. I): 85–88.

Saberi, A., Chen, B. M. & Sannuti, P. (1993). *Loop Transfer Recovery, Analysis and Design*, Springer.

Mattson S.E. (1984). *Modeling and Control of Large Horizontal Axis Wind Power Plants*, PhD thesis, Lund Institute of Technology, Lund, Sweden.

Selvam, K. (2007). Individual pitch control for large scale wind turbines.

Waltz, E. (2008). Offshore wind may power the future, *Scientific American* .

Wilson, D. G., Berg, D. E., Barone, M. F., Berg, J. C., Resor, B. R. & Lobitz, D. W. (2009a). Active aerodynamic blade control design for load reduction on large wind turbines, *European Wind Energy Conference and Exhibition, 16-19 March*.

Wilson, D. G., Berg, D. E., Barone, M. F., Berg, J. C., Resor, B. R. & Lobitz, D. W. (2009b). Active aerodynamic blade control design for load reduction on large wind turbines, *AWEA Wind Power Conference* .

Wilson, D. G., Berg, D. E., Resor, B. R., Barone, M. F. & Berg, J. C. (2009). Combined individual pitch control and active aerodynamic load controller investigation for the 5mw upwind turbine, *AWEA Wind Power Conference* .

Wright, A. D. (2004). Modern control design for flexible wind turbines, *Technical report*, National Renewable Energy Laboratory.

Wright, A. D. & Fingersh, L. J. (2008). Advanced control design for wind turbines part i: Control design, implementation, and initial tests, *Technical report*, National Renewable Energy Laboratory.

Wright, A. & Stol, K. A. (2008). Designing and testing controls to mitigate dynamic loads in the controls advances research turbine, *Conference Paper 2008 ASME Wind Energy Symposium* .